

Relative frequencies of supernovae types: dependence on host galaxy magnitude, galactocentric radius and local metallicity

S. Boissier¹ and N. Prantzos²

¹ Laboratoire d'Astrophysique de Marseille, OAMP, Université Aix-Marseille & CNRS UMR6110, 38 rue Frédéric Joliot Curie, 13388 Marseille cedex 13, France; e-mail: samuel.boissier@oamp.fr

² Institut d'Astrophysique de Paris, UMR7095 CNRS, Univ. P. & M. Curie, 98bis Bd. Arago, 75104 Paris, France; e-mail: prantzos@iap.fr

Submitted, 2008

ABSTRACT

Context. Stellar evolution theory suggests that the relationship between number ratios of supernova (SN) types and metallicity holds important clues as to the nature of the progenitor stars (mass, metallicity, rotation, binarity, etc).

Aims. We investigate the metallicity dependence of number ratios of various SN types, using a large sample of SN along with information on their radial position in, and magnitude of, their host galaxy.

Methods. We derive typical galaxian metallicities (using the well known metallicity-luminosity relation) and local metallicities, i.e. at the position of the SN; in the latter case, we use the empirical fact that the metallicity gradients in disk galaxies are \sim constant when expressed in dex/ R_{25} .

Results. We confirm a dependence of the $N(Ibc)/N(II)$ ratio on metallicity; recent single star models with rotation and binary star models with no rotation appear to reproduce equally well that metallicity dependence. The size of our sample does not allow significant conclusions on the $N(Ic)/N(Ib)$ ratio. Finally, we find an unexpected metallicity dependence of the ratio of thermonuclear to core collapse supernovae, which we interpret in terms of the star formation properties of the host galaxies.

Key words. (stars:) supernovae: general

1. Introduction

The classification of supernovae in various types (II, Ib, Ic, Ia) is based on the presence of various features in their spectra: the presence or absence of hydrogen distinguishes SNII from SNI, while within the SNI family, the presence of Si lines characterizes SNIa and the presence of He lines distinguishes SNIb from SNIc (see e.g. Hamuy 2002, Turatto 2003 and references therein). While SNIa are observed in all types of galaxies (ellipticals, irregulars, spirals), SNIb and Ic (collectively called SNIbc in this work including SN with types Ib, Ic and Ib/c), as well as SNII are only observed in star forming regions of spirals and irregulars; for that reason, they are thought to originate from massive stars, as a result of the gravitational collapse of their Fe cores (gravitational SN or core collapse SN, CCSN in the following). Various schemes have been proposed to relate each one of those types to a progenitor star, either within the framework of single star models (e.g. Heger et al. 2003, Maeder and Meynet 2004) or invoking binary star evolution (e.g. Eldridge et al. 2008).

A comprehensive summary of our current understanding of the various CCSN types is provided in Fryer et al. (2007). Among the various factors affecting the surface chemical composition of a massive star at the time of its explosion, mass, metallicity, rotation and binarity appear to play an important role, while the potential impact of others (e.g. magnetic fields) is not sufficiently explored yet. The extent to which each one of the aforementioned factors (as well as their combined action) determines the mass

lost by the star and its final surface composition is the subject of intense theoretical and observational investigation. In the framework of single star models, it is believed that, for a given metallicity, the lowest mass progenitors of CCSN give rise to SNII, stars more massive than some (yet poorly known) limit M_{Ib} give rise to SNIb and stars more massive than M_{Ic} end as SNIc. In principle, a lower metallicity increases both M_{Ib} and M_{Ic} , but its effect may be compensated by rotation, which mixes nucleosynthesis products from the core to the surface.

In one of the the first attempts to determine empirically the role of metallicity in shaping the various CCSN types, Prantzos and Boissier (2003, PB03 in the following) studied the relationship between the number ratio of SNIbc to SNII $N(Ibc)/N(II)$ vs. the typical metallicity of the host galaxy. In the absence of relevant metallicity measurements, they used the galaxian luminosity as a proxy for metallicity, taking advantage of the well known metallicity-luminosity relation.

Assuming reasonable values for the slope of the IMF (in the -1.30 to -1.70 range), PB03 used the observed global ratio of $N(Ibc)/N(II)$ to derive $M_{Ibc} \sim 20$ -24 M_{\odot} . This mass is comparable to the maximum mass for type II-P SN found by Smartt et al. 2009 in their volume limited sample: $16.5 \pm 1.5 M_{\odot}$ for a Salpeter IMF (and up to 22 M_{\odot} for a steeper IMF). PB03 argued that this value is much lower than the one provided by non-rotating models of single star evolution, even at high metallicity ($>30 M_{\odot}$, e.g. Heger et al. 2003). They suggested instead that rotating models,

such as the solar metallicity models of Meynet and Maeder (2003) offer an appealing solution. Furthermore, PB03 established a correlation of $N(Ibc)/N(II)$ with metallicity (albeit with large error bars) and they attributed it to the fact that M_{Ibc} (the limiting mass between SNII and SNIbc) decreases with metallicity Z . In the absence of relevant models at lower metallicities at that time, PB03 deduced the required $M_{Ibc}=f(Z)$ relationship, in order to fit the observational data (again, for reasonable values of the IMF slope). Subsequent models of low Z massive rotating stars (Maeder and Meynet 2004) confirmed relatively well those quantitative predictions. Recently, similar observational results have been obtained for the $N(Ibc)/N(II)$ vs Z relation by Prieto et al. (2008), who used not the mass-metallicity relation but directly measured metallicities of a smaller sample of host galaxies from the SDSS data base. In the meantime, Eldridge et al. (2008) proposed non-rotating models for binary star evolution, the results of which reproduce also satisfactorily the $N(Ibc)/N(II)$ vs metallicity relation. We shall discuss those theoretical developments in Sec. 5.

In this work, we investigate the relation between metallicity and number ratios of various SN types with a much larger SN sample than PB03 (Sec. 2). We extend our study to the ratios of $N(Ic)/N(Ib)$ and, for the first time, to $N(Ia)/N(CC)$. Furthermore, we derive not only global (typical) galaxian metallicities (Sec. 3) but also local ones, i.e. at the position of the SN within its host galaxy. For that purpose we use the fact that metallicity gradients appear to have a constant value when expressed in dex/R_{25}^1 (Sec. 4). We are thus able to establish statistically significant correlations with both global and local metallicity of $N(Ibc)/N(II)$ and, somewhat surprisingly, of $N(Ia)/N(CC)$. We discuss those findings in Sec. 5 and we summarize our work in Sec. 6.

2. The supernova sample

We use a recent version of the Asiago Supernova Catalogue (presented in Barbon et al. 1999) to obtain information on a large number of supernovae and their host galaxies. This information concerns the SN type, magnitude (usually the discovery magnitude) and relative distance to the galactic center, the galaxy type and various parameters, like position angle, inclination, R_{25} radius and heliocentric radial velocity V_{HEL} . We use the LEDA database (Paturel et al. 2003) to obtain for each galaxy the B-band absolute magnitude M_B . From this list, we keep only galaxies with morphological types corresponding to spirals (S0 to Sd) and irregulars (Irr) as we are interested in the ratio of the various supernovae types occurring in star forming galaxies.

Because of differences in their intrinsic luminosities, various supernovae types can be detected at different distances. In particular, SN Ia are intrinsically brighter than core collapse SN and can be detected further away. Fig. 1 (three top panels) shows the SN magnitude as a function of V_{HEL} in our sample. We are aware that these SN magnitudes are not perfectly well determined, and not always comparable to each other (discovery vs peak magnitude, different photometric bands, no actual distance) but, overall, they give a rough idea of the brightness of the event. The

curves indicate the average and $\pm 1\sigma$ values. They are obtained by computing statistics within the indicated bin size at many points along the x-axis; the distances between those points is less than the bin size, i.e. the points are not independent. We also include four independent points along the curves with errorbars. The grey shaded area indicates the absolute magnitude for SN fainter than 19 magnitudes, where very few SN are found. This value corresponds roughly to the limiting magnitude of SN surveys, especially the LOSS SN Survey (van den Bergh et al. 2005) providing a large number of SN each year. Although the Asiago catalogue does not procure a very well defined sample, we can consider that 19 is our approximate limiting magnitude. Since the various SN types do not have the exact same absolute magnitude, we have to ensure that within the volume we use, we do not miss some types while detecting others. In order to check this, we use the absolute magnitudes (and observation dispersion) given by Richardson et al. (2002) for various types: -16.61 (1.23) for SNII; -17.23 (0.62) for SNIbc; -19.16 (0.76) for Ia. These values are given in their Table 1 and correspond respectively to normal SN II-P, normal Ibc and normal Ia. II-P is the most common type among SNII. Other types (IIn, IIL) are on average brighter, thus if there is no bias against II-P, there should be no bias against SNII either. We note that Richardson et al. (2002) find evidence for a bimodal distribution of the magnitudes of SNIbc, with a brighter component than the normal one. Here again, if we choose our sample in such a way to include all normal SNIbc, we should not be biased against the brighter ones. As long as the average $\pm 1\sigma$ values of Richardson et al. (2002) do not cross the grey-shaded area, the majority of the SN should be present in the catalogue. Fig. 1 thus show that we may miss significant amount of events for SNII, SNIbc, SNIa respectively beyond $V_{HEL} \sim 5000, 9000, 20000$ km/s. Thus, in order to avoid biasing our sample against or in favor of one of the SN subtypes, we have to cut it at $V_{HEL} < 5000$ km/s. Richardson et al. (2006) produced absolute magnitudes for Ib and Ic, respectively -17.98 (scatter of 0.46), and -18.14 (0.48) for the so-called “normal” ones. These values are similar and slightly brighter than the “normal Ibc” taken from Richardson et al. (2002), so SNIb and SNIc should not be biased against each other, neither against SNII adopting $V_{HEL} < 5000$ km/s. Note that here and in the rest of the paper, SN classified as Ib/c are included when computing $N(Ibc)$, but are omitted when computing the ratio $N(Ib)/N(Ic)$.

It can be seen in Fig. 1 that our SNIbc and SNIa are on average fainter than the absolute magnitude given by Richardson et al. (2002). This is likely due to the fact that no extinction corrections are applied to the Asiago values which correspond moreover to discovery magnitudes that may differ from peak magnitudes (the effect is less important for SN II-P which have about constant magnitudes for longer time than Ia or Ibc, making peak and discovery magnitudes closer to each other).

Because the Asiago catalogue is quite inhomogeneous and in view of the afore mentioned magnitudes limits, we checked the robustness of our results by performing our analysis for samples defined in a slightly different ways. Especially, we adopted a more conservative approach, defining a sample with $V_{HEL} < 2000$ km/s. This sample should be less affected by any residual bias but suffers from lower statistics. We also checked the issue that older SN could be

¹ The R_{25} radius is the radius of the 25 mag arcsec⁻² B-band isophote.

misclassified by performing our analysis with the restriction of taking only events that occurred during and after the year 2000 at the price of a smaller number of events and larger error-bars. This affects mostly the trend found for $N(Ia)/N(CC)$ as we will discuss in sections 3.2, 4.1, 4.2.

Richardson et al.(2002) note that about 20% of SN may be sub-luminous (with large uncertainties on this number). Of course, if the same fractions applies to all subtypes, our results would be unchanged. However, we should not consider results to be very robust whenever the obtained trends could be ascribed to a variation in the number of a sub-type by this amount.

Another possible source of bias in SN host studies is the Shaw(1979) effect, i.e. the difficulty in detecting SN in inner parts of distant galaxies, especially in photographic plates searches. This effect depends on the SN search programs (and is thus hard to quantify for the Asiago catalogue) however van den Bergh (1997) considers that it can be neglected for $\log(V_{HEL}) < 3.4$. Our conservative sample ($V_{HEL} < 2000$ km/s) should thus be relatively unaffected. Cappellaro et al.(1993) state that within the same velocity limit ($V_{HEL} < 2000$ km/s), 18% of all SNe are lost in the Asiago/Crimea searches in the overexposure of the central area of galaxies. If all of the lost SN are from one type, the maximum error due to this effect on a ratio is thus 18% in the $V_{HEL} < 2000$ km/s sample. Cappellaro et al.(1993) gives 23% of lost SN for $V_{HEL} < 4000$ km/s and 35% for their whole sample. These numbers are based on the SN missed in photographic searches, assuming CCD/Visual surveys did not miss any of the SN in the central regions. Thus, they could underestimate the real effect. However, we can consider they provide a first guess of the uncertainty on the ratios (especially those derived from the SN radius) due to the Shaw(1979) effect. A trend will be considered robust if it creates a gradient larger than this uncertainty.

In the bottom panel of Fig. 1, we show the $N(Ibc)/N(II)$, $N(Ib)/N(Ic)$, and $N(Ia)/N(CC)$ ratios within the volume defined by V_{HEL} . The intersection with the vertical lines at 5000 (2000) km/s gives the number indicated in Table 1 for our adopted sample (and the ‘‘conservative’’ sample). It is interesting to note that the $N(Ibc)/N(II)$ and $N(Ib)/N(Ic)$ ratios do not depend strongly on the velocity limit adopted. This confirms that we do not miss a large fraction of SNII vs SNIbc (and SNIb vs SNIc) within our samples² (this may be not so surprising as the average absolute magnitudes differ by relatively small amount: -17.23 ± 0.62 vs -16.61 ± 1.23 and -17.98 ± 0.46 vs -18.14 ± 0.48). The ratios $N(Ib)/N(Ic)$, and $N(Ibc)/N(II)$ are thus quite robust, at least in the local universe³. On the contrary, the $N(Ia)/N(CC)$ ratio continuously increases when including more distant SN (i.e. going from $V_{HEL} < 2000$ km/s to $V_{HEL} < 5000$ km/s). Although the limitation at $V_{HEL} < 5000$ km/s should still allow us to derive meaningful results, we note that this ratio does depend on the adopted limit and should thus be considered as relatively uncertain.

² In the worst case scenario, it would mean that we miss similar fractions of SNII vs SNIbc (and SNIb vs SNIc) when we push the velocity limit to larger values

³ Since the $N(Ibc)/N(II)$ ratio depends on metallicity (PB03) and since cosmic metallicity decreases, on average, with redshift, that ratio is expected to decline with redshift, albeit very slowly.

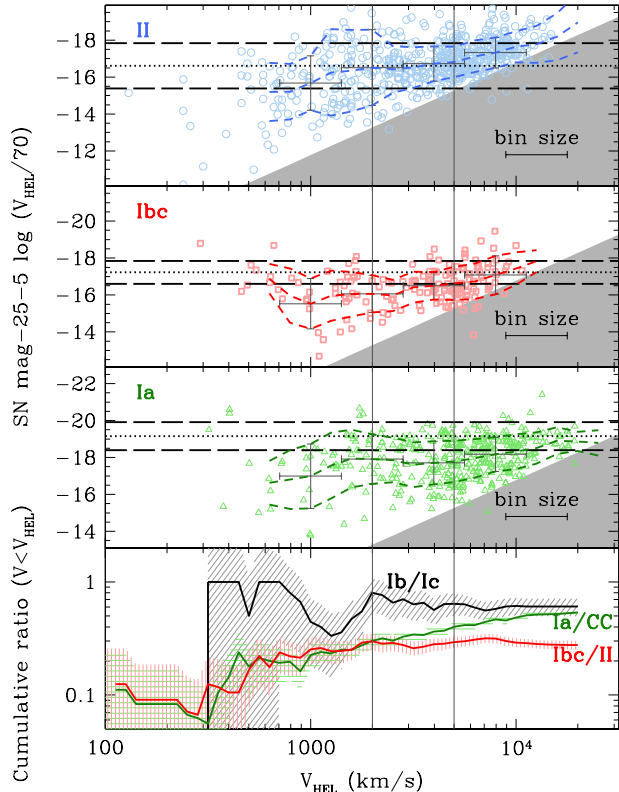


Fig. 1. *Top* three panels: Supernovae absolute magnitude (adopting a basic Hubble’s law with $H_0 = 70 \text{ km/s Mpc}^{-1}$) as a function of the heliocentric velocity, for SN of type II, Ibc and Ia, respectively (from top to bottom). The curves show the average (*solid*) and 1σ dispersion (*dashed*) within bins of size indicated in the bottom-right part of the figure (only points separated by a distance larger than the bin size are independent in these curves, see text). Independent points with error bars are also displayed in each panel. The *dotted* (and *long-dashed*) lines show the average magnitude (and its dispersion) given in Richardson et al.(2002). Almost no SN are found in the shaded area (apparent magnitudes fainter than 19) because it corresponds roughly to the limiting magnitude of the sample (see text). *Bottom*: Cumulative ratios of SN types vs heliocentric velocity. *All panels*: the 2 vertical lines indicates the two velocity limits for which we present results : 5000 km/s (excluding distant galaxies for which we start missing large numbers of type II SN), and the more conservative 2000 km/s.

Adopting $V_{HEL} < 5000$ km/s, the catalogue provides 1038 SN, 701 occurring in star forming galaxies (spirals and irregulars) and for which we have at least the host galaxy magnitude. The sample we will use to study the core-collapse ratios is then a factor 2.5 larger than the 280 CCSN used in PB03. The distribution of SN types in this sample is given in Table 1.

The SN ratios that we obtain for the different SN types of our sample are consistent with published values: the ratio of SNIbc to SNII supernovae in our sample is $N(Ibc)/N(II) = 0.31 \pm 0.04$, similar to 0.27 in PB03; 0.23 ± 0.05 in Bressan et al. (2002); 0.33 in Hamuy (2002); 0.41 in Smartt et al. (2009), 0.3, 0.16 and 0.31 for re-

Table 1. Size of the samples and ratios

SN Type	Larger statistics $V_{HEL} < 5000$ km/s	Conservative $V_{HEL} < 2000$ km/s
Ic	49 (41)	18 (15)
Ib	32 (25)	15 (12)
Ibc	98 (79)	43 (36)
II	318 (239)	142 (96)
Ia	166 (132)	56 (42)
$N(Ibc)/N(II)$	0.31 ± 0.04 (0.06)	0.30 ± 0.05 (0.06)
$N(Ic)/N(Ib)$	1.53 ± 0.35 (0.30)	1.20 ± 0.42 (0.24)
$N(Ia)/N(CC)$	0.40 ± 0.04 (0.08)	0.30 ± 0.05 (0.06)

Top part : The first number is the number of SN of a given type for which at least the magnitude of the host is available, the second number (between parenthesis) is the number of SN for which the position of the SN relative to the center of the galaxy is also known. Bottom part: SN ratios computed from the first of the two numbers above, with statistical error. The data between parenthesis indicates what would be a 20% error resulting from missing systematically under-luminous SN from one of the subtypes; it is also the order of magnitude of the Shaw(1979) effect for $V_{HEL} < 2000$ km/s (see text).

spectively S0a/b, Sbc/d and Irr galaxies in Mannucci et al. (2005). The ratio of thermonuclear to core collapse SN in that sample is $N(Ia)/N(CC)=0.4\pm 0.04$, and the same ratio is obtained from the local universe supernovae sample (Smartt et al. 2009). Using the rates from Mannucci et al. (2005), we obtain for that ratio the values 0.41, 0.19, and 0.34 in S0a/b, Sbc/d, and Irr galaxies, respectively; the corresponding uncertainties, however, are very large, due to small statistics. Our result for $N(Ic)/N(Ib)=1.65 \pm 0.32$ is consistent with the one obtained from the local universe sample of Smartt et al. (2009): $N(Ic)/N(Ib)=2$ considering the small statistics (27 SN) in their sample for this ratio (compensated however by a careful checking of the data for every SN used in their work).

3. Dependence of SN type ratios on global galaxy properties

Using a sample of 280 CCSN from an earlier version of the Asiago catalogue, PB03 found that the $N(Ibc)/N(II)$ ratio has an average value of ~ 0.30 , while it increases with host galaxy magnitude. They interpreted the latter as an effect of the global galaxian metallicity (increasing with galaxian luminosity) on the masses of the precursors of the CCSN sub-types: as metallicity increases, the stellar envelope is more easily lost and lower mass stars may become SNIbc, increasing thus the $N(Ibc)/N(II)$ ratio. Assuming all CCSN are produced from single stars, and that the physical reason for a star to explode as a SNIc, SNIb, SNIi is only its initial mass (see the discussion in section 5 for other possibilities), the $N(Ibc)/N(II)$ ratio is expressed as

$$\frac{N(Ibc)}{N(II)} = \frac{\int_{M_{Ibc}}^{M_{Up}} \Psi(t - \tau_M) \Phi(M) dM}{\int_{M_{II}}^{M_{Ibc}} \Psi(t - \tau_M) \Phi(M) dM} \quad (1)$$

where $\Psi(t)$ is the star formation rate at time t , τ_M the lifetime of star of mass M , $\Phi(M)$ the stellar initial mass function (IMF), and M_{Up} , M_{II} and M_{Ibc} , respectively, the upper mass limit of the IMF (around $100 M_{\odot}$), the lower mass limit for a star to explode as SNIi (around $8 M_{\odot}$, see

e.g. Smartt et al. 2009, Anderson & James 2008) and the lower mass limit for a star to explode as SNIbc. Under the crucial assumption of stationarity, whereby the progenitor lifetimes of both classes of SN (i.e. SNIi and SNIbc) are short compared to the duration of the corresponding star formation episodes, Ψ can be taken out of the integral in Eq. (1) and cancelled (since the progenitors of both classes of SN have similar lifetimes, during which Ψ varies very little). Then, Eq. (1) reads:

$$\frac{N(Ibc)}{N(II)} = \frac{\int_{M_{Ibc}}^{M_{Up}} \Phi(M) dM}{\int_{M_{II}}^{M_{Ibc}} \Phi(M) dM} \quad (2)$$

i.e. the $N(Ibc)/N(II)$ ratio is a function of the slope of the IMF and of M_{Ibc} . For a given IMF, if M_{Ibc} increases with metallicity, the ratio given by Eq. (2) will obviously decrease and the same is true if one replaces $N(Ibc)/N(II)$ with $N(Ic)/N(Ib)$ and M_{Ibc} with M_{Ic} . Note that Anderson & James(2008) recently suggested such a hierarchy of limiting masses between SNIi, SNIb, SNIc on the basis of the association of SN with regions of recent star formation traced by H α emission. Their findings indicate $M_{II} \sim 7.8 M_{\odot}$. Kelly et al.(2008) found that SNIc occur in the brightest regions of their host, where the most massive stars probably form, also suggesting that SNIc results from the explosion of the most massive stars.

3.1. The $N(Ibc)/N(II)$ and $N(Ic)/N(Ib)$ ratios

In this section we first repeat the analysis as PB03 for the ratios of CCSN subtypes with our larger sample. In Fig. 2, the top panels show the $N(Ibc)/N(II)$ ratio vs M_B . Four bins in M_B with ~ 100 CCSN in each one are constructed and the corresponding M_B value is taken as the median value of M_B in each bin. In can be seen in the insert panel that in bins of constant CCSN numbers, $N(Ibc)$ increases for brighter galaxies ($N(II)$ decreasing by the same amount), making the $N(Ibc)/N(II)$ ratio to increase with galaxian luminosity. The resulting $N(Ibc)/N(II)$ vs M_B relation is quite similar to the one obtained in PB03 (dotted curve), with smaller vertical error bars, reflecting the larger size of the new sample. We thus confirm the original result of PB03 between the $N(Ibc)/N(II)$ ratio and *global* galaxian metallicity, which is also supported by the study of Prieto et al. (2008). The only limitation to this conclusion is obtained with the conservative sample for which the relation is rather flat. The main difference come from the bin corresponding to the brightest galaxies showing low values with respect to the $V_{HEL} < 5000$ km/s sample and the PB03 fit (errorbars are however rather large). We shall return to the interpretation of that result in Sec. 5, after presenting in Sec. 4 the results of our study concerning that same ratio as a function of *local* metallicity.

The $N(Ic)/N(Ib)$ ratio (middle panel of Fig. 2) has considerably larger uncertainties than the $N(Ibc)/N(II)$ ratio, because of poorer statistics. Indeed, each one of the four bins contains ~ 8 SNIb and ~ 12 Ic (insert in middle panel), for an average ratio of $N(Ic)/N(Ib) \sim 1.6$. That ratio shows no clear variation with M_B . At first sight, this appears to indicate a situation opposite to the case of the $N(Ibc)/N(II)$ ratio. We shall see, however, in Sec. 4, that the situation is different when $N(Ic)/N(Ib)$ is expressed as a function of local metallicity. This ‘‘puzzling’’ behaviour is

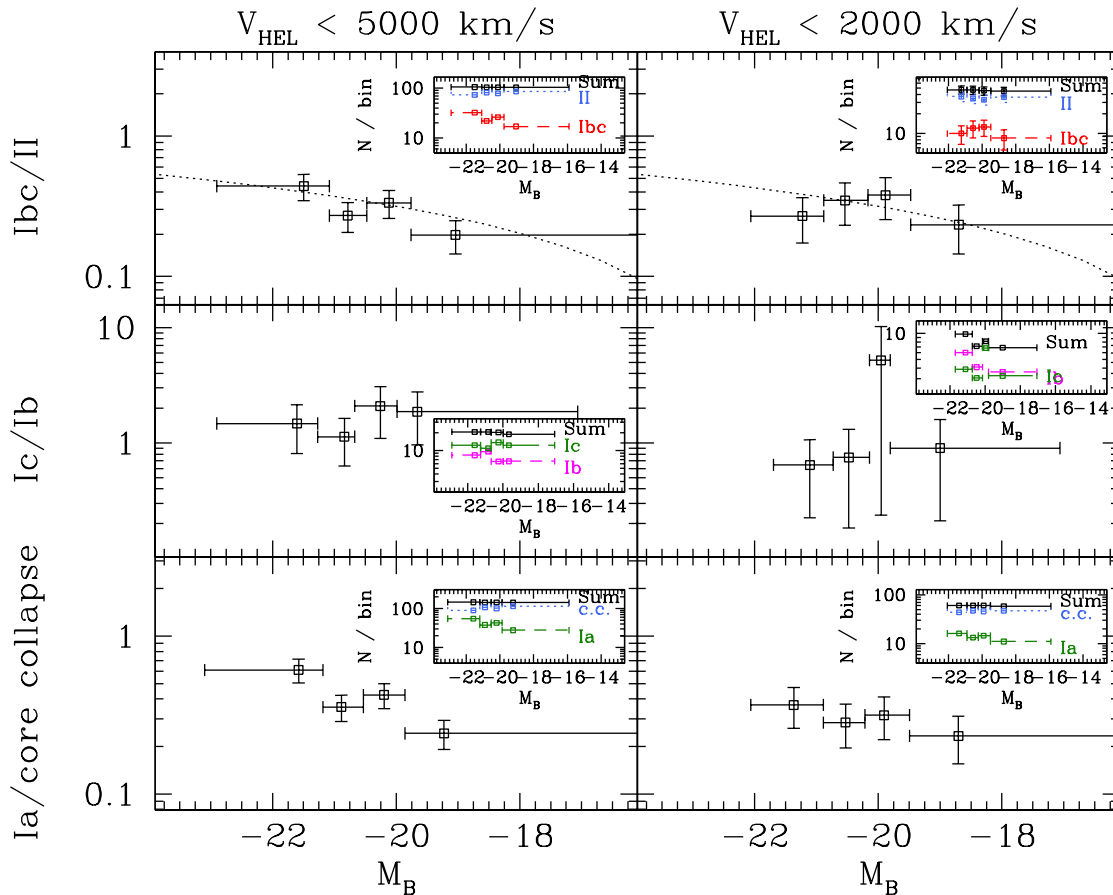


Fig. 2. From *top to bottom*: number ratios of $N(Ibc)/N(II)$, $N(Ic)/N(Ib)$ and $N(Ia)/N(CC)$, as function of galaxian blue magnitude M_B for the conservative $V_{\text{HEL}} < 2000$ km/s sample (*right*) and the $V_{\text{HEL}} < 5000$ km/s sample (*left*, better statistics). The inserts in each panel display the corresponding numbers of each SN type and are chosen such as each M_B bin has the same total number of SN of the types involved. The *dotted* curve in the upper panel is the fit to the data of PB03, which had much larger error bars.

further discussed in Sec. 4 and attributed to small number statistics.

3.2. The $N(Ia)/N(CC)$ ratio

In this section, we extend our study to the $N(Ia)/N(CC)$ ratio as a function of host galaxy M_B . As can be seen in the bottom panels of Fig. 2, there is also a clear trend in that case, with brighter galaxies hosting proportionally more SNIa than CCSN. To our knowledge, it is the first time that such a correlation is put in evidence. In view of the numbers of SN involved (see insert panel) we feel that this result is rather robust, contrary to the case of $N(Ic)/N(Ib)$. We note that we still find such a correlation for the conservative limit $V_{\text{HEL}} < 2000$ km/s (right panel) although it is less steep in that case. On the other hand, taking only recent SN from the sample (trying to avoid misclassifications), the correlation gets steeper. The dependence of $N(Ia)/N(CC)$ on the magnitude is thus relatively uncertain in absolute value, however the fact that we do find a correlation with magnitude in every one of our tests let us think that it is real.

That result can be translated in terms of metallicity, with larger $N(Ia)/N(CC)$ ratios found in more metal-rich galaxies. We shall see indeed in Sec. 4 that this result also

holds when the local metallicity is considered. However, we think that, contrary to the previous case, there is no causal relationship here, i.e. metallicity does not affect in any way the $N(Ia)/N(CC)$ ratio. Instead, it is the mass of the host galaxy which affects that ratio, in a way that can most easily be seen as follows.

The CCSN rate of a galaxy is proportional to the star formation rate Ψ :

$$N(CC) \propto \Psi \quad (3)$$

The SNIa rate is more difficult to evaluate, since thermonuclear supernovae may result from stars of all ages, not just the young ones. Scannapieco and Bildsten (2005) introduced a useful parametrization, describing the SNIa rate as a sum of two terms, one depending on the current star formation rate and the other on the total stellar mass M_* (i.e. the time integrated star formation rate). That parametrization (adopted by e.g. Sullivan et al. 2006, Aubourg et al. 2008) fits satisfactorily most available data and we adopt it here:

$$N(Ia) = \alpha \Psi + \beta M_* \quad (4)$$

where α and β are constants. Thus, the required ratio can be written as

$$\frac{N(Ia)}{N(CC)} = A + B \frac{M_*}{\Psi} \quad (5)$$

Now, it is well known that larger galaxies have, on average, smaller specific star formation rates Ψ/M_* because of their smaller gas fractions (e.g. Boissier et al. 2001; Boissier and Prantzos 2000 and references therein), i.e. the ratio M_*/Ψ is, on average, an increasing function of galaxy mass and luminosity. Thus, both the metallicity of a galaxy and its $N(Ia)/N(CC)$ ratio increase with its mass. This explains, at least qualitatively, the correlation found in the bottom panels of Fig. 2.

4. Dependence of SN type ratios on local galaxy properties

PB03 used the absolute magnitude of the host galaxy as a proxy for its global metallicity, based on the well established magnitude-metallicity relationship. However, disk galaxies are known to exhibit metallicity gradients (e.g. Henry and Worthey 1999, Zaritsky et al. 1994, van Zee et al. 1998). If metallicity affects indeed the ratios of SN types, a radial effect should also be found. Hakobyan (2008) has indeed shown that the radial distributions of SNIbc and SNII are different, with more SNIbc found at smaller radii than SNII (using a sample extracted from the Asiago catalogue also, but with a different selection than ours), A similar analysis was made by van den Bergh (1997), for a smaller sample of 156 SN.

4.1. Dependence on galactocentric distance

In this section we investigate whether such a radial effect is seen in our sample, using the supernovae for which we can compute a galactocentric radius. This is possible when the catalogue provides the offset of the SN, the position angle and inclination of the host galaxy, as well as its R_{25} radius, which is needed to normalize the results. From these parameters, we compute the distance between the SN position and the center of the galaxy, within its plane, that we will call the galactocentric radius of the SN. Note that we de-project the minor axis simply as $b/a = \cos(\text{inclination angle})$, and we do not use the galaxies which are almost edge-on (inclination larger than 80 degrees). These restrictions reduce the size of the usable sample for this part of the study, but only moderately (see Table 1) allowing us to work with decent statistics.

Fig. 3 displays the same ratios as Fig. 2, this time as a function of galactocentric radius. A clear trend is observed in the case of $N(Ibc)/N(II)$. SNIbc are found at smaller normalised radius than SNII, in agreement with Hakobyan (2008). van den Bergh (1997) already suggested from his small sample that SN Ibc were more concentrated toward the central part of their host galaxy than SNII. As mentioned in section 2, the Shaw(1979) effect should be lower than 35%, but the difference between the inner and outer bins is much larger (about a factor 2.5). Actually adopting the conservative sample (right panel), the Shaw(1979) effect should be even smaller, and we still find a trend (actually, even stronger: slope of -0.85 instead of -0.71). Thus we believe this trend to be unaffected by this source of bias. The easiest way to interpret this observation is in term of metallicities: larger metallicities are found in inner parts of galaxies, leading to a lower limiting mass for type Ibc supernovae. We shall quantify the effect in Sec. 5.2 in terms of local metallicities, showing that it is

consistent with what we obtained in Sec. 4 by using global metallicities.

The clear trend obtained in the case of $N(Ic)/N(Ib)$ (middle panels in Fig. 3) is rather surprising, in view of the results of Sec. 2: $N(Ic)/N(Ib)$ apparently increases with decreasing galactocentric radius (i.e. with increasing metallicity) while no variation with M_B is seen in Fig 2. We note that with a difference between inner and outer bins of a factor about 5, here again, we cannot ascribe the observed trend to the Shaw(1979) effect (if we adopt the conservative sample, we do not have any SN Ib in the inner most bin, but the trend in the three other bins is stronger). We attribute the striking difference between the trend with magnitude and radius to the small number statistics involved in the evaluation of that ratio. As stressed in the beginning of Sec. 4, the assumption of stationarity is crucial in the evaluation of the various SN ratios. That assumption is naturally fulfilled if large numbers of SN are involved. In that case, the formation times of the SN progenitors of all types span the whole range of the progenitor lifetimes (τ_M); an average Ψ can be used then, allowing one to pass from Eq. (1) to Eq. (2). However, in the case of small numbers of SN the situation is different: if a few starbursts occurred recently (less than a few Myr ago), only the most massive of their stars had time to explode up to now, favouring SNIc (presumably resulting from more massive stars) over SNIb (and, for the same reasons, SNIbc over SNII). In that case, the term $\Psi(t - \tau_M)$ in Eq. (1) does not cancel out with the corresponding term in the denominator and may mask the effect of any metallicity dependence of M_{Ibc} (the dividing mass between SN exploding as Ibc or II) or of M_{Ic} (the dividing mass between SN exploding as Ib or Ic). We shall see in the next section that the radial trend of $N(Ic)/N(Ib)$ found here translates directly into a local metallicity trend, but because of low number statistics it is impossible to draw meaningful conclusions.

Finally, the bottom panels of Fig. 3 displays the ratio of thermonuclear to core collapse supernovae $N(Ia)/N(CC)$. The ratio appears to increase in the inner galaxian zones. The trend is relatively weak: with the slope and uncertainty in the figure, a Student's t-test indicates a 20% probability for the null hypothesis that there is no dependence of $N(Ia)/N(CC)$ on the radius. Very similar results are obtained for the conservative sample ($V_C < 2000$ km/s). Another worrying issue is that inner and outer bins are different only by a factor ~ 1.4 . This is still larger than the typical uncertainties due to the Shaw(1979) effect or underluminous SN, but in combination with the large statistical error-bars, it makes this trend less robust vs uncertainties than the other ones presented in the figure. Interestingly, if we keep only SN that exploded during or after the year 2000, avoiding possible misclassifications for older SN, we find a steeper trend with radius (slope -0.46 ± 0.06 , reducing the probability for the null hypothesis to less than 1%). In summary, although the trend in Fig. 3 is not very strong, it is reasonable to believe it is real in the sense that we still find it when reducing the size sample with various criteria aiming to improve its quality. It is rewarding that such a trend is also expected on the basis of the analysis made in Sec. 3.2. Indeed, the gaseous profiles of disk galaxies vary little with galactocentric radius, while the stellar ones much more (for instance, in the case of the Milky Way disk the scalelength of the stellar profile is ~ 2.5 kpc, while the one of the gas ~ 8 kpc; see e.g. Boissier and Prantzos

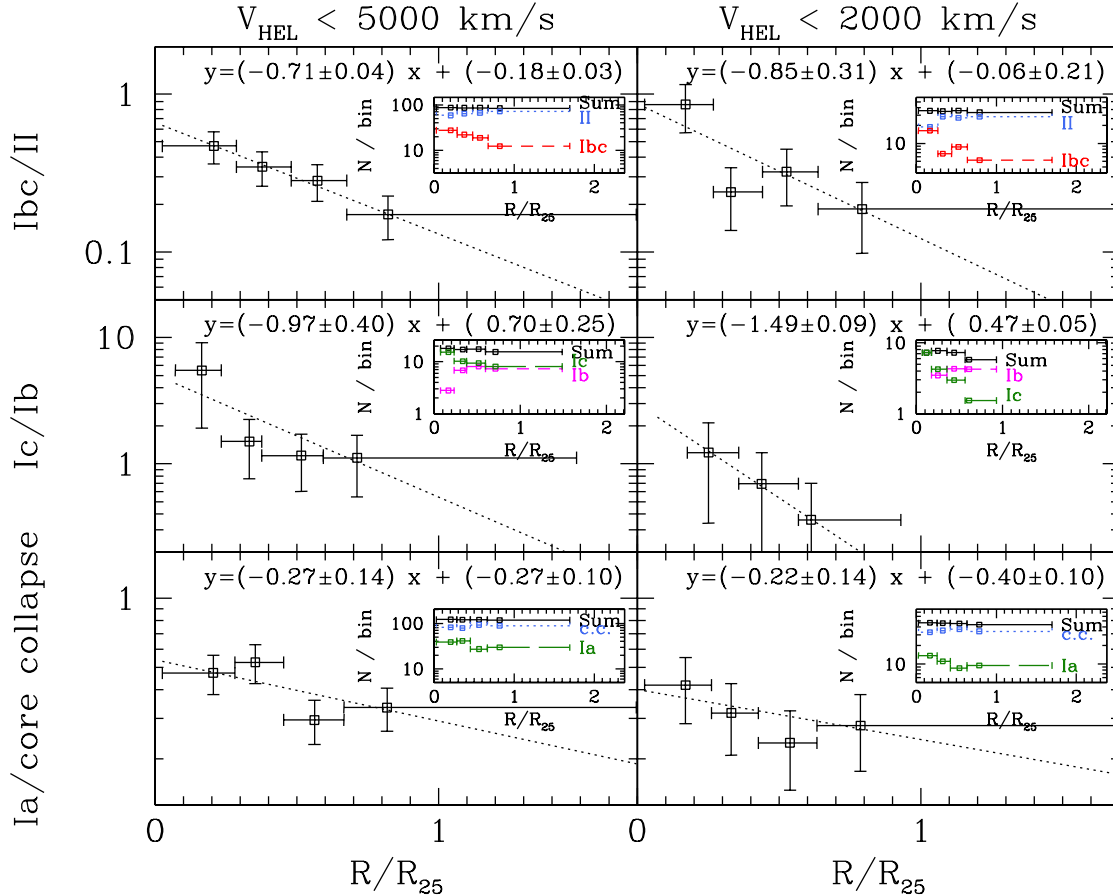


Fig. 3. Same thing as in Fig. 2, but this time as a function of galactocentric radius, expressed in units of R_{25} .

1999 for observed stellar and gaseous profiles of the MW disk). This implies that the term M_*/Ψ in Eq. (5) is expected to increase in the inner galaxian zones and so will do the corresponding $N(Ia)/N(CC)$ ratio. We develop further this argument analytically in Sec. 5.3 and we illustrate it with a numerical example from the case of the Milky Way disk. We shall see in the next section that this radial trend is also expressed in terms of local metallicity; however, as already argued in Sec. (2), metallicity is not the root cause of that effect.

4.2. Dependence on local metallicity

In order to probe the metallicity dependence of SN types, one may use direct or indirect methods to determine metallicity. Direct measurements of abundances of host galaxies of supernovae are possible only for moderately large samples of SN (e.g. 254 galaxies from the SDSS in Prieto et al., 2008) and these are integrated abundances over the whole galaxy, not at the supernova position. Measuring local metallicities, i.e. in HII regions at the immediate vicinity of the supernova, would be ideal but it would require an enormous observational effort before numbers for decent statistics are obtained. Determinations of local metallicities from spectroscopy of neighboring HII regions do exist (Smartt et al. 2009, Modjaz et al. 2008) but only for relatively small number of events, not allowing the statistical study of the various trends explored in this work.

In PB03 we used an indirect way, i.e. the well-known mass-metallicity relationship to evaluate the metallicity of the host galaxies (of late type) of CCSN. In this work, we use known relationships among disk galaxies in order to derive again in an indirect (and approximate) way the local metallicity of galaxies at the galactocentric radius of the supernovae of our sample.

It is known that the abundance gradient in nearby disk galaxies has a universal value when expressed in dex/R_{25} (e.g. Henry and Worthey, 1999) of $d\log(O/H)/dR_{25} \sim -0.6 \text{ dex}/R_{25}$. Prantzos and Boissier (2000) showed, with detailed semi-analytical models of disk galaxy evolution, that this universality can indeed be reproduced, thus confirming an earlier suggestion of Garnett et al. (1997) on “homologous” disk evolution. Combining this empirical fact with the observed luminosity-metallicity relation, it is possible to deduce the metallicity at the vicinity of the SN from the luminosity of the host galaxy and the galactocentric radius of the SN (which is already evaluated in Sec. 4.1).

For our purpose we use the data of two studies of abundance gradients with relatively large samples of nearby galaxies : Zaritsky et al. (1994) and van Zee et al. (1998). We show in Fig. 4 (top) the abundance gradients in dex/R_{25} , which display little variation (if any at all) with absolute magnitude. In the bottom panel of Fig. 4 is displayed the abundance measured at $0.4 R_{25}$ as a function of the absolute B band magnitude M_B (the metallicity-luminosity relation). Each panel features a linear least square fit for these relationships (solid lines) that we adopt

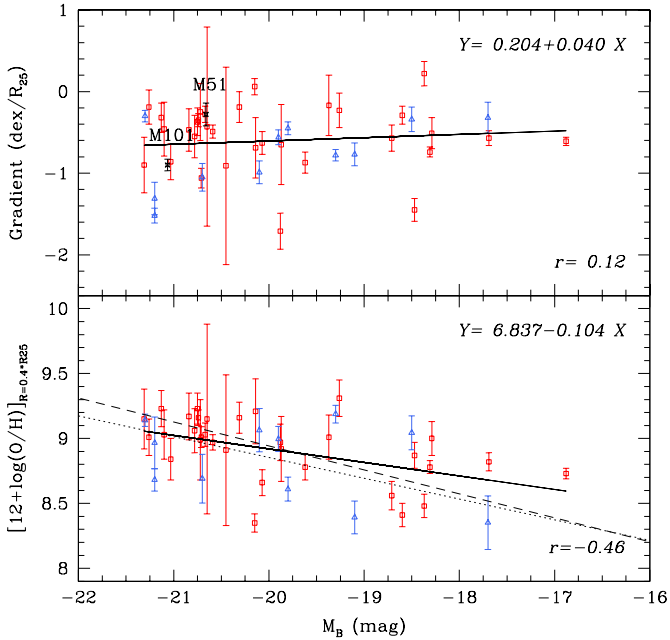


Fig. 4. *Top:* Metallicity (oxygen) gradient per R_{25} as a function of absolute magnitude M_B . *Bottom:* Characteristic metallicity (at $0.4 R_{25}$) as a function of M_B . Data in both panels are from Zaritsky et al. (1994) (squares) and van Zee et al. (1998) (triangles). r is the correlation coefficient, and the *solid* line indicates in each case the best linear least squares fit (the parameters of the line are given in each panel). In the top panel, the gradients recently derived by Bresolin et al. (2004) and Bresolin (2007) for M51 and M101 are overplotted. In the bottom panel, *dashed* and *dotted* lines indicate, respectively the empirical relations obtained by Tremonti et al. (2004) and Garnett (2002) using respectively global metallicities (measured on the integrated galaxy spectra) and metallicities at the effective (half-light) radius. The latter was used as a proxy for the global metallicity in PB03. We apply the same approach in this paper for the global metallicity.

in this work to compute the local metallicity. The dashed and dotted lines in the bottom panel of Fig. 4 indicate the metallicity-luminosity relations of Tremonti et al. (2004) and Garnett (2002). The first one was obtained from integrated galaxy spectra of the Sloan Digital Sky Survey. The second one displays the metallicity at the effective (half-light) radius and was used in PB03 to estimate the metallicity in SN hosts without knowing the galactocentric distance of the SN. In this paper, for consistency, we still use it to estimate the global metallicity. Despite using different definitions of the “characteristic” abundance, the aforementioned relationships are very close to each other, and our results would be marginally affected by the use of either of them.

Assuming that the two empirical relations (i.e. the solid lines in the top and bottom panels) are valid for all the galaxies of our sample, we can compute the metallicity profile (in terms of R/R_{25}) of each galaxy from its luminosity. We can then evaluate easily the local metallicity at the galactocentric radius of the supernova. Using the numerical values of Fig. 4 (i.e the fits appearing in each panel) we

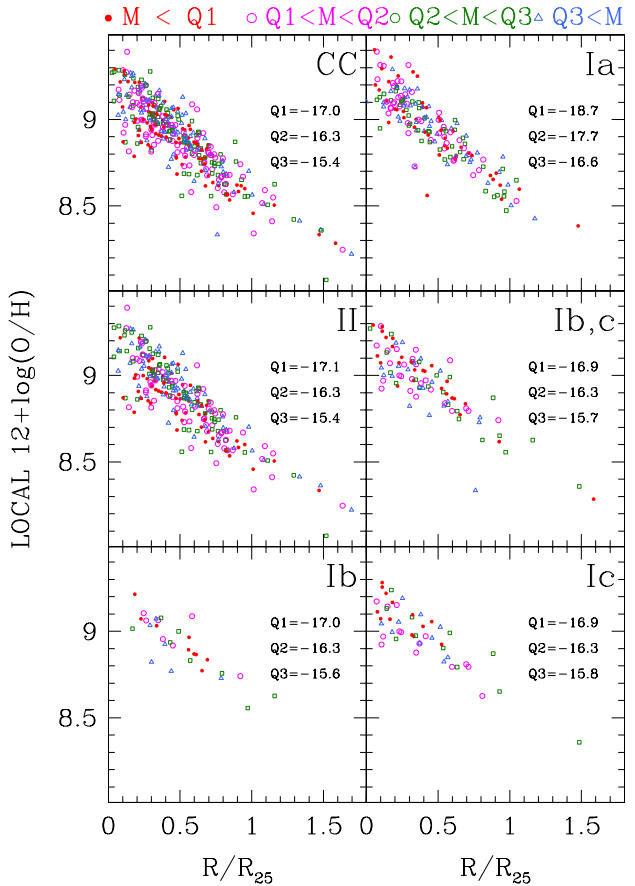


Fig. 5. Metallicities of the various SN types of our sample, as a function of their position (expressed in R/R_{25}) inside their host galaxy. Metallicities are derived from the SN position in and the magnitude of the host galaxy, according to the procedure described in Sec. 5.2 and Eq. 6. The color/type coding is done according to the absolute magnitude of the SN with respect to the three quartiles Q1, Q2, Q3 indicated in each panel.

obtain:

$$[12 + \log(O/H)](R) = 6.837 - 0.104 M_B + \left(\frac{R}{R_{25}} - 0.4\right)(0.204 + 0.04 M_B) \quad (6)$$

Notice that, although the abundance gradient has an almost universal value in dex/R_{25} , our fit provides a very small trend with M_B , which appears as the last term (dependence on M_B) in the derived expression. We keep this term for consistency, but it is clear that, in view of its small magnitude, it has no influence on the results.

The resulting local metallicities $O/H(R)$ as a function of normalized galactocentric radius R/R_{25} appear in Fig. 5 for all the SN of our sample: the upper panels displays CCSN and SNIa, the middle panels SNIb and SNIbc and the bottom panels SNIb and SNIc. In all cases, the metallicity gradient is the same, but the absolute value of the metallicity at each normalized radius depends on the corresponding host galaxy magnitude. It is the first time that this technique is used in order to derive local metallicities for SN progenitors. Its results depend obviously on how accurately the adopted *average* relationships (metallicity-

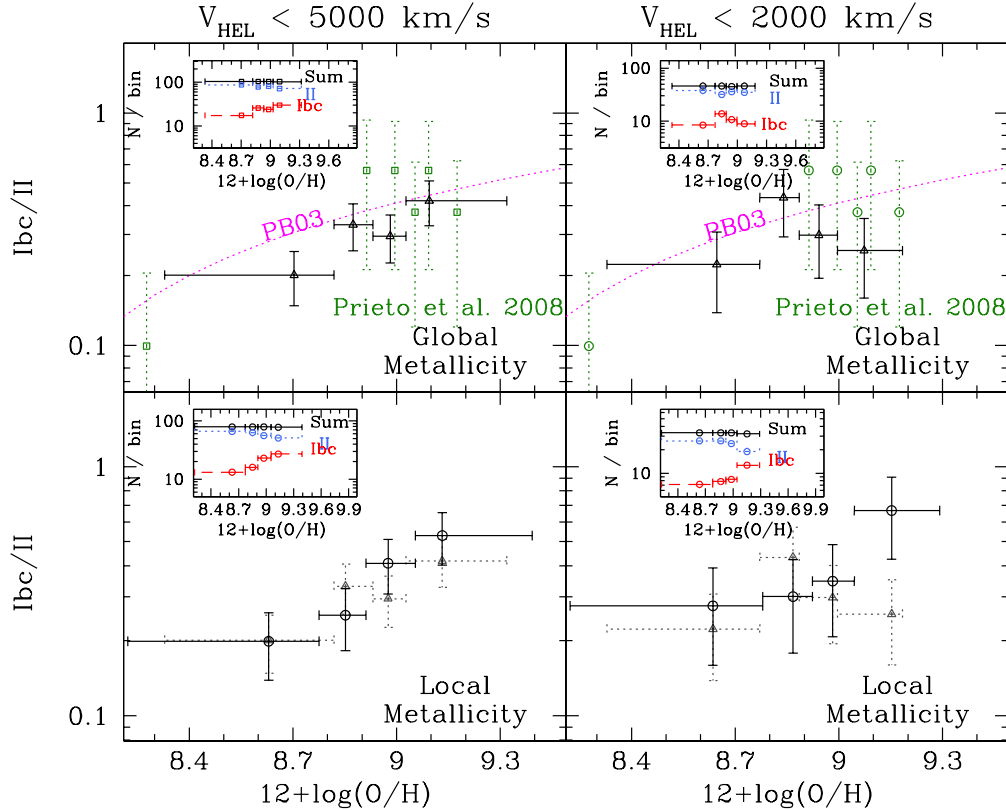


Fig. 6. Symbols with *solid error bars*: Number ratios of SNIbc/SNII as a function of global galaxian metallicity (*top*, obtained from the magnitude-metallicity relation of Fig. 4) and of local metallicity (*bottom*, obtained from Eq. 6), for the conservative $V_{HEL} < 2000$ km/s sample (*right*) and the $V_{HEL} < 5000$ km/s sample (*left*, better statistics). Inserts in all panels display corresponding numbers of SN in each bin (chosen such as the total numbers are approximately equal). *Triangles with dotted error bars* in lower panels are the same as those with *solid error bars* in the upper panels and are displayed for comparison with local metallicity results. In the *upper* panels, the *dotted curve* is the fit to the data of PB03 and the symbols with *dotted vertical error bars* the data collected in Prieto et al. (2008).

luminosity and gradient-luminosity) apply to each galaxy of our sample.

With the metallicities at the position of each supernovae derived in this way, we compute then the corresponding ratios as a function of the local metallicity. In Fig. 6 and Fig. 7, we present the results for respectively the ratios $N(Ibc)/N(II)$ and $N(Ic)/N(Ib)$ as a function of global metallicity (top, after the results of Sec. 4.1 and the magnitude-metallicity relationship) and of local metallicity (bottom).

Before discussing these results, we want to mention that we performed the same figure adopting different abundance gradients. During the last years, several studies have mentioned the possible errors in the abundances obtained from strong lines as in Zaritsky et al. (1994) or van Zee et al. (1998). Bresolin et al. (2004) and Bresolin (2007) performed a more detailed analysis of the gradients in M51 and M101. They found flatter gradients than in previous studies for the same galaxies, however their gradients are within the dispersion of those in Fig. 4. We performed the same analysis as described above but adopting the two values for M51 and M101 rather than our fit. We find that it does not affect our results qualitatively. The only difference is that flatter gradients make the trend with metallicity steeper and vice versa.

In the case of $N(Ibc)/N(II)$, the results of the $V_{HEL} < 5000$ km/s as a function of global metallicity are consistent with those obtained in PB03 (dotted curve) and those of Prieto et al. (2008, vertical dotted error bars). We note the relatively good statistics, due to the size of our sample (see insert). The corresponding ratios as a function of local metallicity (bottom panel) are quite consistent with those obtained for global metallicity and the statistics is almost equally significant. Looking at the $V_{HEL} < 2000$ km/s sample, we notice that the trend with global metallicity is consistent with an absence of relationship. However, this is mostly due to the higher metallicity bin (the three other ones are indeed within 1 sigma of the PB03 fit). We think that small statistics are partly responsible for this difference. The relation with local metallicity however (that should be a better estimator of the actual progenitor metallicity) is totally consistent with the one obtained with the $V_{HEL} < 5000$ km/s sample. We conclude then that the trend of $N(Ibc)/N(II)$ with metallicity, first identified in PB03, is firmly established as long as the two types Ibc and II are unbiased as a function of R/R_{25} . The discussion in section 4.1 suggests that it is the case. Also, in Fig. 5, the symbol/color coding according to the SN magnitudes shows that SN in the inner galactic regions are not apparently biased towards the brighter ones. The case of $N(Ic)/N(Ib)$ is much less clear. Results show no trend with global metal-

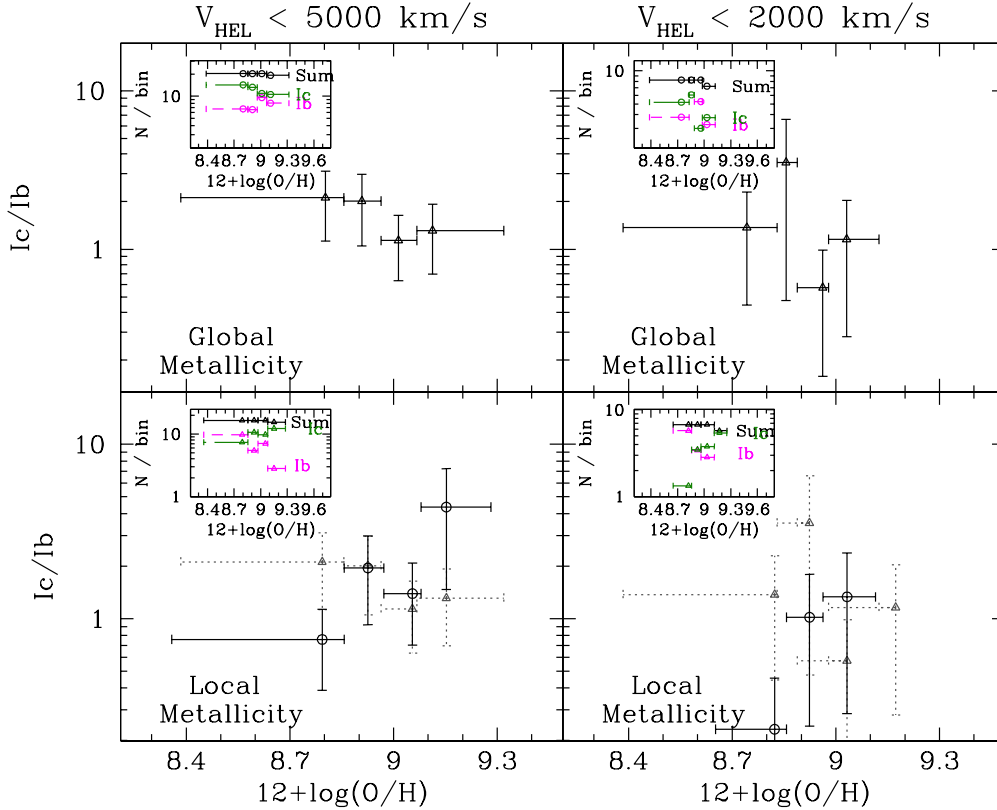


Fig. 7. Symbols with *solid error bars*: Number ratios of SNIc/SNIb as a function of global galaxian metallicity (*top*, obtained from the magnitude-metallicity relation of Fig. 4) and of local metallicity (*bottom*, obtained from Eq. 6), for the conservative $V_{HEL} < 2000$ km/s sample (*right*) and the $V_{HEL} < 5000$ km/s sample (*left*, better statistics). Inserts in all panels display corresponding numbers of SN in each bin (chosen such as the total numbers are approximately equal). *Triangles with dotted error bars* in lower panels are the same as those with *solid error bars* in the upper panels and are displayed for comparison with local metallicity results.

licity (as expected from Sec. 3.1) but they do show such a trend as a function of local metallicity (as expected from Sec. 4.1), even if the slope and intercept are poorly constrained (see the error-bars and the difference between the two samples shown in Fig. 7) Due to the smaller samples (see inserts) statistics is poorer in that case, as reflected in the large error bars. The arguments developed in Sec. 4.1 suggest that such a conflicting situation can occur indeed: Eq. 2 does not apply and Eq. 1 (which always applies) can produce ambiguous results, depending on the ages of the few starbursts involved. It is then impossible to draw any conclusions about the dependence of that ratio on metallicity; a substantially larger sample is required for that.

Finally, our results for the SNIa/CCSN ratio are plotted in Fig. 8 as a function of global (top) and local (bottom) metallicities. Results are plotted for the two samples with values of the maximal heliocentric velocities of the host galaxies $V_{HEL} < 2000$, and 5000 km/s. The left and right panels show respectively the results using all the SN, or only the recent ones. It is clearly seen that:

i) For global metallicities, the slope of the relation differs in the two sample defined by different maximal velocity by quite a large amount. This reflects the difference mentioned in section 3.2 for the $N(\text{Ia})/N(\text{CC})$ ratio as a function of the magnitude. We note that if we restrict ourselves to recent SN (right part of Fig. 8), the data from the 2 samples ($V_{HEL} < 2000$, and 5000 km/s) get within

error-bars from each-other (these error-bars are however large). This suggests misclassifications do play a role in our $N(\text{Ia})/N(\text{CC})$ ratio and the slope of the relation is quite uncertain. However, in any cases, we do find a correlation.

ii) The same tendency is obtained for local metallicities. We note that, although the number of SNIa in each bin is rather small (see inserts for the case of $V_{HEL} < 2000$ km/s) the lifetimes of the progenitors of SNIa are quite long, in general, and thus we have not the problem described in the previous paragraphs for the SNIc/SNIb ratio (the more so, since the numbers of CCSN in each bin are quite substantial). Here again, very similar trends are obtained restricting ourselves to recent SN (even if large statistical error-bars make the slope less significant, especially for the $V_{HEL} < 2000$ km/s sample). The variation of the ratio within the whole range of metallicity is larger than the uncertainties (mentioned in section 2) due to the Shaw(1979) effect, or the presence of sub-luminous SN. We conclude then that the trend of increasing SNIa/CCSN ratio with metallicity is likely to be real, although the relation between the SNIa/CCSN ratio and metallicity still carries large uncertainties.

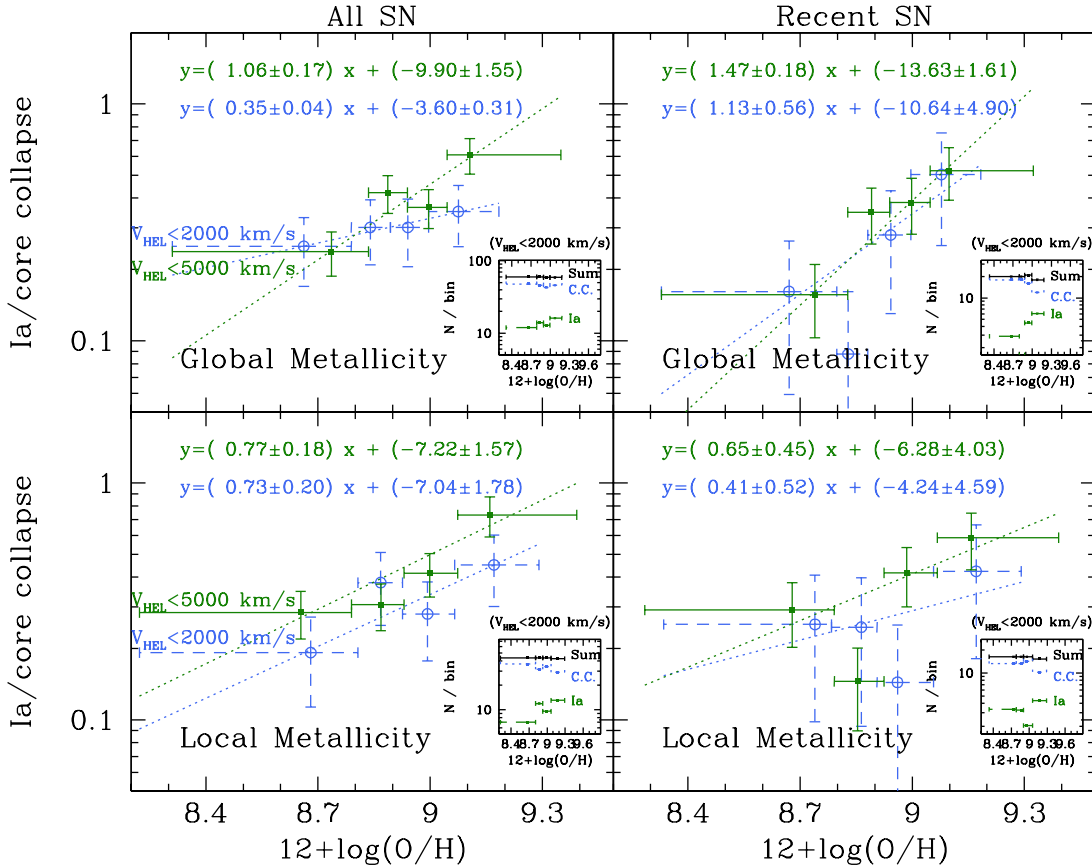


Fig. 8. Number ratio of SNIa/CCSN as a function of global (*top*) and local (*bottom*) galaxian metallicity. Data are displayed (left panels) for our two samples adopting various maximal heliocentric velocities V_{HEL} of the host galaxies: 2000 km/s (*dashed*), and 5000 km/s (*solid*). The same is shown in the right panels but keeping only recent SN (events that occurred during and after 2000).

5. Discussion

5.1. The $N(Ibc)/N(II)$ ratio

The variation of $N(Ibc)/N(II)$ ratio with metallicity is quite well established now (PB03, Prieto et al. 2008 and this work). Equally well established is the fact that non-rotating single star models can reproduce neither the observed trend nor the average value of that ratio. This is clearly seen in Fig. 9, where recent results of Eldridge et al. (2008) are plotted (*long dashed curve*).

As suggested in PB03, single star models with rotation are promising in that respect. In Fig. 9 we present results of such models from the Geneva group (Maeder and Meynet 2004, *dot-dashed curve*; Meynet et al. 2008, *dotted curve*). They are both obtained for a power-law IMF with slope $x=-1.35$. Their behaviour is compatible with observational data, especially if observational error bars are taken into account.

An even better fit to the data is obtained by the recent binary star models of Eldridge et al. (2008). This result is somewhat surprising, since it is not *a priori* obvious how metallicity can affect to such extent the evolution of stars in binaries. Eldridge et al. (2008) argue that high metallicity favors a more extended envelope for massive stars and, in the case of close binary systems, more extended envelopes

make easier the loss of mass through Roche lobe overflow into the secondary.

In view of those results, it appears difficult to decide whether stellar rotation or binary evolution is at the origin of the observed trend. Theoretical uncertainties are quite important in both cases (but certainly more in the case of binary evolution), making it premature to draw firm conclusions. It may well be that both factors contribute to the observed trend.

Stellar models predict the metallicity dependence of M_{Ibc} (the minimum mass for a single star to lose its hydrogen envelope); then, folding with a stellar MF allows one to calculate the resulting $N(Ibc)/N(II)$ ratio vs. metallicity, as e.g. in Fig. 9. Inversely, observed $N(Ibc)/N(II)$ ratio vs. metallicity can be used to evaluate M_{Ibc} vs. metallicity. This was done for the first time in PB03, who predicted the metallicity dependence of M_{Ibc} on the basis of then available data for $N(Ibc)/N(II)$ vs. metallicity. In Fig. 10 we present the result of PB03 (thin solid curve) and of our new evaluation (thick solid curve) for a slope $x=-1.35$ of the IMF. The two curves are close to each other and not very different from the theoretical predictions of Meynet et al. (2008, *dotted curve*) at low metallicities. Notice that, in order to compare the results of Meynet et al. (2008), expressed as a function of Z/Z_{\odot} , to our own which are expressed as a function of O/H , we assume that

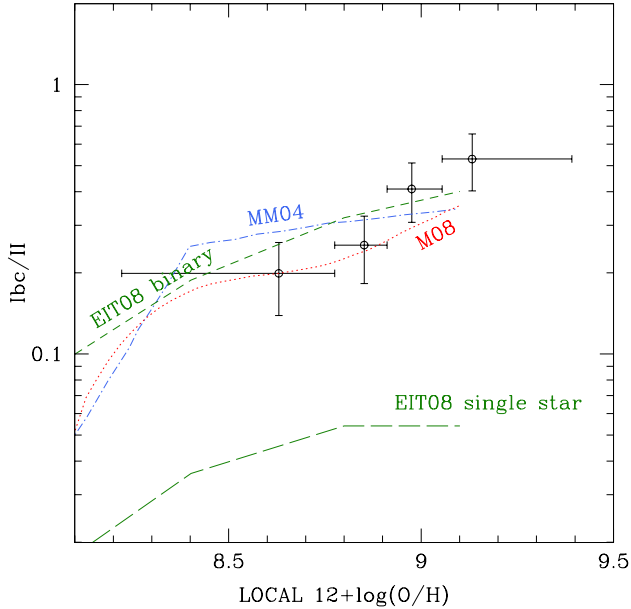


Fig. 9. Number ratio of SNIbc/SNII as a function of local galaxian metallicity and comparison to single star rotating models of Maeder and Meynet (2004, MM04, *dot-dashed*) and of Meynet et al. (2008, M08, *dotted*), single non-rotating stellar models of Eldridge et al. (2008, EIT08, *long dashed*) and binary non-rotating stellar models of Eldridge et al. (2008, EIT08, *short dashed*).

the solar oxygen abundance is $\log(\text{O}/\text{H})_{\odot}+12=8.8$; this value is close to the one determined recently for the Sun $\log(\text{O}/\text{H})_{\odot}+12=8.76\pm 0.007$ (Caffau et al. 2008). At high metallicities observationally determined M_{Ibc} is systematically lower than the predictions of Meynet et al. (2008), but by only a couple of solar masses. Notice that the theoretical predictions of M_{Ibc} are independent of the IMF, while the empirical determinations do depend on it: a steeper IMF would produce a M_{Ibc} vs. metallicity curve lower by a few solar masses than the one shown in Fig. 10. Inversely, the theoretical $N(Ibc)/N(II)$ ratio vs. metallicity does depend on the IMF: a steeper IMF would produce $N(Ibc)/N(II)$ ratios lower than depicted in Fig. 9.

Given the various uncertainties, our estimates for the minimum mass of SNIbc at solar metallicity are in fairly good agreement with empirical estimates for the minimum mass of WN stars in the Milky Way, which lies in the 20-25 M_{\odot} range (Massey et al. 2001, Massey 2003, Crowther 2007).

5.2. The $N(Ic)/N(Ib)$ ratio

In the case of $N(Ic)/N(Ib)$ ratio, the observational situation is not clear at present, since different trends are obtained as a function of global and local metallicity; we argued in the previous section that small number statistics are at the origin of this dichotomy. One may only determine a global value of $N(Ic)/N(Ib) \sim 1.6$, i.e. there are about 50% more SNIc than SNIb. Fryer et al. (2007) find that this high ratio is “... against intuition in the single star case and it may be a further argument in favor of binary origin for SNIc”. However, a simple evaluation of the

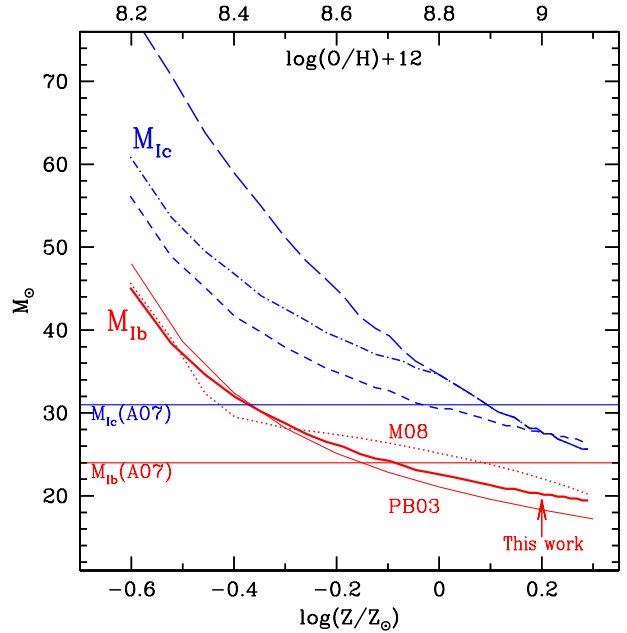


Fig. 10. Minimum mass for single stars becoming SNIb or SNIc as a function of metallicity, according to theoretical and empirical evaluations. The two *horizontal lines* are from Arbutina (2007), based on measured global SNIbc/CCSN and SNIc/SNIb ratios. The three lower curves are for M_{Ib} , from theoretical (Meynet et al. 2008, *dotted*) and empirical evaluations (PB03, *thin solid* and this work *thick solid*). Finally, the three upper curves are for M_{Ic} from this work, assuming that the M_{Ib} vs metallicity curve of this work is correct and that the IMF extends up to $100 M_{\odot}$. The three curves are obtained then assuming that: i) the SNIc/SNIb ratio is 1.6, as in upper left panel in Fig. 7 (*short dashed*), ii) the SNIc/SNIb ratio depends on metallicity as in lower left panel in Fig. 7 extrapolated below the lowest observed metallicity (*long dashed*), and iii) the SNIc/SNIb ratio depends on metallicity only for $Z > Z_{\odot}$ and remains equal to unity below solar (*dot-dashed*). The two metallicity scales match each other for $\log(\text{O}/\text{H})_{\odot}+12=8.8$.

limiting masses on the basis of global observations and for a Salpeter IMF with slope $x=-1.35$ gives $M_{Ib}=24 M_{\odot}$ and $M_{Ic}=31 M_{\odot}$ (Arbutina 2007), i.e. it is easy to obtain the observed ratio if it is assumed that SNIb originate from a limited range of masses (between 24 and $31 M_{\odot}$, with more massive stars exploding as SNIc).

From the theoretical point of view, there is a dearth of predictions for $N(Ic)/N(Ib)$ even for the single star case. It is generally assumed that SNIc originate from more massive stars than SNIb. However, there is no agreement on the amount of He left in the envelope for a star to explode as SNIc. Moreover, although it is generally agreed that the most massive stars end up in black holes, it is not clear what happens when a black hole is formed: is a bright optical display still obtained, or is the explosion underluminous or even failed (see e.g. Fryer et al. 2007 and references therein)? In the latter case, the upper part of the IMF would not contribute to SNIc and the $N(Ic)/N(Ib)$ ratio could be small.

For illustration purposes we present in Fig. 10 three curves for the mass limit M_{Ic} as a function of metallicity,

on the basis of various assumptions about the true observational trend. We assume that the stellar IMF extends up to $100 M_{\odot}$ and that the results of this work for M_{Ib} (*thick solid curve* in Fig. 10) are correct. The slope of the IMF plays little role in the resulting M_{Ic} and we shall consider here only the case of $x=-1.35$ (Salpeter slope). We proceed by considering three possible cases for the variation of $N(Ic)/N(Ib)$ ratio with metallicity, on the basis of the results presented in Fig. 7.

i) $N(Ic)/N(Ib)=\text{constant} = 1.6$ (upper left panel in Fig. 7). This leads to the lowest of the three curves for M_{Ic} in Fig. 10 (*short-dashed curve*): the curve runs almost parallel to the one for M_{Ib} , at a “distance” of a $6-10 M_{\odot}$, i.e. SNIb are produced only for a limited range of stellar masses running from 45 to $55 M_{\odot}$ at the lowest metallicities and from 20 to $26 M_{\odot}$ at the highest metallicities.

ii) $N(Ic)/N(Ib)=Z/Z_{\odot}$ at all metallicities (lower left panel of Fig. 7, trend extrapolated to lower than solar metallicities). In that case we obtain the highest lying curve in Fig. 10 (*long-dashed*). At low metallicities the ratio is small and the limiting mass M_{Ic} is as high as $75 M_{\odot}$, while at high metallicities we recover the results of the previous case.

iii) $N(Ic)/N(Ib)=Z/Z_{\odot}$ at $Z>Z_{\odot}$ and $N(Ic)/N(Ib)=1$ for $Z<Z_{\odot}$. This case leads to a curve intermediate between the two previous ones (*dot-dashed* in Fig. 10)

The obtained curves confirm the finding of Arbutina (2007) on the basis of global SN ratios, namely that it is possible to have both SNIb and SNIc solely from single star evolution; this suggests that the concern expressed in Fryer et al. (2007) was unfounded. If the $N(Ic)/N(Ib)$ ratio is ~ 2 at high metallicities, then the range of masses producing SNIb is rather limited. This is also found in the single star models with rotation of Meynet et al. (2008), although no quantitative predictions are given. The wide spacing between the curves of M_{Ic} corresponding to cases (i) and (iii) in Fig. 10 suggests that a substantial effort is required in order to pin down the true metallicity dependence of $N(Ic)/N(Ib)$ ratio through better statistics.

5.3. The $N(Ia)/N(CC)$ ratio

In Sec. 3.2 we gave an explanation of the observed variation of $N(Ia)/N(CC)$ ratio with global metallicity. Here we provide a similar argument for the observed variation of $N(Ia)/N(CC)$ ratio with local metallicity. In the case of a star forming galactic disk, Eq. (5) can be rewritten in terms of local surface densities of stars $\Sigma_{*}(R)$ and of star formation rate $\Psi(R) \propto \Sigma_g^k(R)$, where $\Sigma_g(R)$ is the gas surface density at galactocentric distance R and $k=1.4$ the coefficient in the Kennicutt (1998) empirical “star formation law”.

$$\frac{N(Ia)}{N(CC)} = A + B \frac{\Sigma_{*}}{\Sigma_g^k} \quad (7)$$

where all variables depend on radial distance R . Stellar profiles in galactic disks are usually fitted with exponentials of scalelength R_{*} , i.e. $\Sigma_{*}(R) \propto \exp(-R/R_{*})$. Corresponding gaseous profiles are always much flatter than stellar ones and if fitted by exponentials they would be $\Sigma_g(R) \propto \exp(-R/R_g)$ with $R_g > 2R_{*}$. In the case of the Milky Way, for instance, one has $R_{*} \sim 2.5$ kpc and $R_g \sim 8$ kpc; further

examples for external disk galaxies can be found in e.g. Boissier et al. (2003). Eq. (7) is then rewritten as

$$\frac{N(Ia)}{N(CC)} = A + C \exp\left(-\frac{R_g - kR_{*}}{R_g R_{*}} R\right) \quad (8)$$

where C is a new constant. It is clearly seen that, for reasonable values of k (< 2), the expression (8) is a decreasing function of radius R . Thus, in galactic disks it is expected that the $N(Ia)/N(CC)$ ratio will increase towards the inner galaxy, i.e. it will be correlated to metallicity, as observed.

We illustrate this behaviour in Fig. 11, where we plot the relevant quantities for the case of the Milky Way disk. All curves are obtained from an updated successful model of the Galactic disk (from Boissier and Prantzos 1999). For the SNIa rate, the formalism by Greggio and Renzini (1983) is adopted in the model and the corresponding results are displayed with *solid* curves in all panels. We also apply the simple analytic expression of Eq. (8) and the corresponding results are plotted with *dotted* curves. Fig. 11 displays the present-day ($T=12.5$ Gyr) radial profiles of CCSN, SNIa and gas fraction (top left panels), the profiles of $N(Ia)/N(CC)$ ratio and oxygen (bottom left panels) and shows clearly that both $N(Ia)/N(CC)$ and metallicity increase at lower gas fractions, i.e. in the inner disk (top right panel). Finally, in the bottom right panel we show that the resulting $N(Ia)/N(CC)$ vs metallicity relation compares favorably with the data of Fig. 8; the analytical prescription for the SNIa rate leads to a more steeply rising $N(Ia)/N(CC)$ ratio with metallicity than the prescription of Greggio and Renzini (1983), but in both cases the agreement with observations is satisfactory. Obviously, an increase of the observational sample of SN will allow in the future to reduce error bars and to constrain prescriptions for the SNIa rate.

6. Summary

In this work we derive relationships between ratios of various SN types and metallicity of host galaxies. For that purpose we determine either global metallicities (reflecting the composition at radius $R = 0.4 R_{25}$) or local ones, i.e. at the position of the SN inside the host galaxy. In the former case we use the well known metallicity-magnitude relationship, a technique applied already in PB03 (albeit with a smaller SN sample). In the latter case, we use the fact that galaxian metallicity gradients appear to be \sim constant when expressed in dex/R_{25} ; this method is applied for the first time, to our knowledge, to the determination of local metallicities in disks and appears quite promising. We made a number of tests, defining several samples and using different values for the abundance gradients, in order to make sure the observed trends are not biased.

We find that $N(Ibc)/N(II)$ ratio increases with both global metallicity (as already found in PB03 and in Prieto et al. 2008) and with local one. Our study reduces considerably error bars of previous works. We consider this result as established now (the variation of $N(Ibc)/N(II)$ with metallicity is larger than the changes that could cause any biases we can think of, and the trend is consistently obtained for almost all our samples, e.g. with various assumptions or limits on V_{HEL} , with the exception of the $V_{HEL} < 2000$ km/s sample in which the ratio for the higher *global* metallicity bin is lower than expected for such a trend) and we

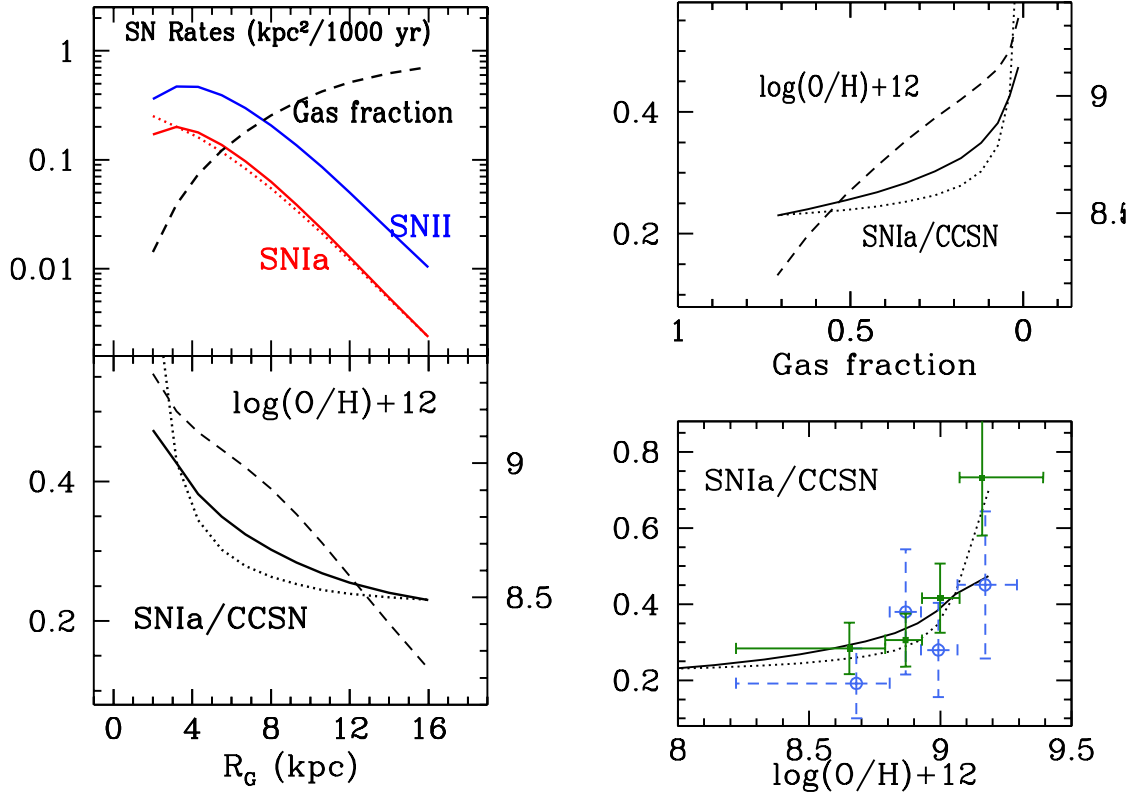


Fig. 11. Illustration of the variation of SNIa/CCSN ratio as a function of metallicity, with a realistic model of galactic evolution (from Boissier and Prantzos 1999). *Top left:* Rates of CCSN (*solid*) and SNIa (*solid*: model, *dotted*: analytical) and gas fraction (*dashed*) as a function of galactocentric radius. *Bottom left:* SNIa/CCSN ratio (*solid*: model, *dotted*: analytical) and metallicity profile (*dashed*, right vertical axis). *Top right:* SNIa/CCSN ratio (*solid*: model, *dotted*: analytical) and metallicity (*dashed*, right vertical axis). *Bottom right:* SNIa/CCSN ratio (*solid*: model, *dotted*: analytical) as a function of metallicity; comparison is made to the data for local metallicity of Fig. 8 (*bottom-left*).

discuss it in terms of either single star models with rotation or binary evolution models. In view of observational and theoretical uncertainties (certainly larger in the case of binary evolution than in the case of single stars) we find it difficult to chose between the two possibilities. Assuming that only single stars produce SNIbc, we derive the empirical M_{Ibc} vs. metallicity relation and we find it to be compatible with the one obtained with the latest models of the Geneva group (Meynet et al. 2008).

We study the $N(Ic)/N(Ib)$ ratio and we find it consistent with being constant w.r.t. global metallicity but increasing with local one. We attribute this difference to small number statistics and we believe that larger SN samples in the future will allow to distinguish between the two possibilities. Nevertheless, we derive the empirical $M_{Ic}=f(Z)$ relation assuming again that only single stars are at the origin of SNIb and SNIc. We find that this assumption leads to SNIb being produced within a relatively limited range of stellar masses, as found in rotating star models of Meynet et al. (2008). We show that the single star channel can justify $N(Ic)/N(Ib)$ ratios as high as 2 and we disagree in that respect with the concern expressed in Fryer et al. (2007), namely that such a high ratio favours the binary channel for SNIc.

Finally, we find for the first time an unexpected correlation between the ratio of $N(Ia)/N(CC)$ and metallicity, both global and local. Although the precise values

of the slope and intercept are subject to large uncertainties (various samples provide different results), the trend is statistically secure (the null hypothesis has a probability of only 7% using local metallicity and the conservative $V_{HEL} < 2000$ km/s sample). We argue that this is not a causal relationship, contrary to the previous cases; instead, both $N(Ia)/N(CC)$ and metallicity are higher in regions of smaller gas fractions (or lower specific star formation rates). We develop this argument analytically and we illustrate it with a quantitative application to the case of the Milky Way disk.

Comparing to the situation only ~ 6 years ago, we find that the increase of the SN sample size since PB03, and the use of local metallicities rather than global ones allowed us to establish the strong likelihood of the $N(Ibc)/N(II)$ vs metallicity trend. We expect then that a similar increase in the future will allow one to establish the $N(Ic)/N(Ib)$ vs. metallicity trend and to probe with greater accuracy the intricacies of the SNIa rate.

Acknowledgements. We thank S. Basa and T. Zhang for useful discussions. We thank the referee, S. Smartt for his detailed review of the paper and his suggestions. We acknowledge the usage of the HyperLeda database (<http://leda.univ-lyon1.fr>), as well of the Padova-Asiago supernova catalogue, from the Padova-Asiago Supernova Group (<http://web.pd.astro.it/supern/>)

References

- Anderson, J. P., & James, P. A. 2008, *MNRAS*, 390, 1527
- Arbutina, B. 2007, *International Journal of Modern Physics D*, 16, 1219
- Aubourg, E., Tojeiro, R., Jimenez, R., Heavens, A. F., Strauss, M. A., & Spergel, D. N. 2007, accepted in *A&A* (arXiv:0707.1328)
- Barbon, R., Buondi, V., Cappellaro, E., & Turatto, M. 1999, *A&AS*, 139, 531
- Boissier, S., & Prantzos, N. 1999, *MNRAS*, 307, 857
- Boissier, S., & Prantzos, N. 2000, *MNRAS*, 312, 398
- Boissier, S., Boselli, A., Prantzos, N., & Gavazzi, G. 2001, *MNRAS*, 321, 733
- Boissier, S., Prantzos, N., Boselli, A., & Gavazzi, G. 2003, *MNRAS*, 346, 1215
- Bresolin, F. 2007, *ApJ*, 656, 186
- Bresolin, F., Garnett, D. R., & Kennicutt, R. C., Jr. 2004, *ApJ*, 615, 228
- Bressan, A., Della Valle, M., & Marziani, P. 2002, *MNRAS*, 331, L25
- Caffau, E., Ludwig, H.-G., Steffen, M., Ayres, T. R., Bonifacio, P., Cayrel, R., Freytag, B., & Plez, B. 2008, *A&A*, 488, 1031
- Cappellaro, E., Turatto, M., Benetti, S., Tsvetkov, D. Y., Bartunov, O. S., & Makarova, I. N. 1993, *A&A*, 273, 383
- Crowther, P. A. 2007, *ARA&A*, 45, 177
- Eldridge, J. J., Izzard, R. G., & Tout, C. A. 2008, *MNRAS*, 384, 1109
- Fryer, C. L., et al. 2007, *PASP*, 119, 1211
- Garnett, D. R., Shields, G. A., Skillman, E. D., Sagan, S. P., & Dufour, R. J. 1997, *ApJ*, 489, 63
- Garnett, D. R. 2002, *ApJ*, 581, 1019
- Greggio, L., & Renzini, A., 1983, *A&A*, 118, 217
- Hakobyan, A. A. 2008, *Astrophysics*, 51, 69
- Hamuy, M. 2002, in "Core Collapse of Massive Stars", Ed. C.L. Fryer, Kluwer, Dordrecht
- Heger, A., Fryer, C. L., Woosley, S. E., Langer, N., & Hartmann, D. H. 2003, *ApJ*, 591, 288
- Henry, R. B. C., & Worthey, G. 1999, *PASP*, 111, 919
- Kelly, P. L., Kirshner, R. P., & Pahre, M. 2008, *ApJ*, 687, 1201
- Kennicutt, R. C., Jr. 1998, *ApJ*, 498, 541
- Maeder, A., & Meynet, G. 2004, *A&A*, 422, 225
- Mannucci, F., Della Valle, M., Panagia, N., Cappellaro, E., Cresci, G., Maiolino, R., Petrosian, A., & Turatto, M. 2005, *A&A*, 433, 807
- Massey, P., DeGioia-Eastwood, K., & Waterhouse, E. 2001, *AJ*, 121, 1050
- Massey, P. 2003, *ARA&A*, 41, 15
- Meynet, G., & Maeder, A. 2003, *A&A*, 404, 975
- Meynet, G., Chiappini, C., Georgy, C., Pignatari, M., Hirschi, R., Ekstrom, S., & Maeder, A. 2008, arXiv:0810.0652
- Modjaz, M., et al. 2008, *AJ*, 135, 1136
- Paturel, G., Petit, C., Prugniel, P., Theureau, G., Rousseau, J., Brouty, M., Dubois, P., & Cambrésy, L. 2003, *A&A*, 412, 45
- Prantzos, N., & Boissier, S. 2000, *MNRAS*, 313, 338
- Prantzos, N., & Boissier, S. 2003, *A&A*, 406, 259
- Prieto, J. L., Stanek, K. Z., & Beacom, J. F. 2008, *ApJ*, 673, 999
- Richardson, D., Branch, D., Casebeer, D., Millard, J., Thomas, R. C., & Baron, E. 2002, *AJ*, 123, 745
- Richardson, D., Branch, D., & Baron, E. 2006, *AJ*, 131, 2233
- Scannapieco, E., & Bildsten, L. (2005), *ApJ*, 629, L85
- Shaw, R. L. 1979, *A&A*, 76, 188
- Smartt, S. J., Eldridge, J. J., Crockett, R. M., & Maund, J. R. 2009, arXiv:0809.0403
- Sullivan, M., et al. 2006, *ApJ*, 648, 868
- Tremonti, C. A., et al. 2004, *ApJ*, 613, 898
- Turatto M., 2003, in *Supernovae and GRBs*, v. 598 of *Lecture Notes in Physics*, K. Weiler (Ed.), Springer-Verlag, p. 21
- van den Bergh, S. 1997, *AJ*, 113, 197
- van den Bergh, S., Li, W., & Filippenko, A. V. 2005, *PASP*, 117, 773
- van Zee, L., Salzer, J. J., Haynes, M. P., O'Donoghue, A. A., & Balonek, T. J. 1998, *AJ*, 116, 2805
- Zaritsky, D., Kennicutt, R. C., Jr., & Huchra, J. P. 1994, *ApJ*, 420, 87